Reference Signal Design for Remote Interference Management in 5G New Radio

Elena Peralta*, Mikko Mäenpää†, Toni Levanen*,Youngsoo Yuk‡, Klaus Pedersen§, Sari Nielsen¶, Mikko Valkama*
*Department of Electrical Engineering, Tampere University, Finland, †Wireless System Engineering Finland Ltd, Finland
‡Nokia Bell Labs, Republic of Korea, §Nokia Bell Labs, Denmark, ¶Nokia Bell Labs, Finland

***Abstract*—In time division duplexing based mobile networks, under certain atmospheric ducting conditions, the uplink reception may be interfered by the downlink transmissions of remote base-stations (BSs) located hundreds of kilometers away. This paper addresses such remote interference problem in 5G new radio (NR) macro deployment context. Specifically, two potential reference signal (RS) designs for remote interference management (RIM) are described, together with receiver detection processing framework, to efficiently detect the interference due to multiple remote aggressor base-stations.The first signal structure, denoted as the one OFDM symbol (1OS) based RIM-RS, is building on the channel state information reference signals (CSI-RS) of 5G NR. The second candidate is referred to as the two OFDM symbol (2OS) based RIM-RS design, and builds on the design principles of LTE RIM-RS. The considered RIM-RS solutions are extensively analyzed and compared, with different parameterizations, in several realistic interference scenarios. The obtained results show that the 2OS RS design provides better RIM performance in scenarios where the number of interfering BSs is small. However, when the number of interfering BSs increases, the 1OS RS design starts to outperform the 2OS based approach. Additionally, it is shown that the 1OS RIM-RS provides smaller overhead and can be frequency multiplexed with the physical downlink shared channel.**

***Keywords*—5G New Radio (NR), Atmospheric ducting, Remote Interference Management, Reference Signal Design, Physical Layer**

I. Introduction

In the fifth generation new radio (5G NR) mobile networks [1], with time division duplexing (TDD) based macro deployments, the downlink (DL) transmissions from one 5G NR base station (denoted as gNB) may degrade the signal-to-interference-and-noise ratio in the uplink (UL) reception of a remote gNB under certain atmospheric conditions. Such remote interference takes place especially under the so-called atmospheric ducting phenomenon. In general, the atmospheric ducts are horizontal layers commonly found under specific weather conditions in the lower atmosphere, i.e., the troposphere [2], [3]. Typically, the ducting occurs when the radio waves face a higher refractive index in a layer of warm air in the troposphere [4] as illustrated in Fig. 1. In this type of cases, the radio waves experience a bending effect as well as lower propagation loss and they tend to propagate within the duct boundaries for large distances, even hundreds of kilometers. The remote interference also causes a so-called sloping interference-over-thermal-noise power response [5] at the victim gNB, as shown in Fig. 1, where the sloping interference power response over different UL OFDM symbols is caused by accumulated signals from several remote aggressor gNBs or groups of gNBs with different distances.

The development of efficient methods for remote interference management (RIM) has received significant interest,

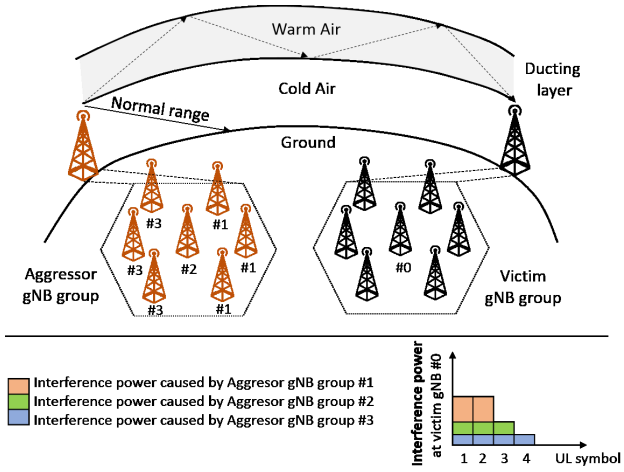

Fig. 1: Illustration of the remote interference problem stemming from the atmospheric ducting phenomenon and related sloping interference power with respect to the UL symbol index.

in general, and particularly in 3GPP 5G New Radio (NR) standardization, see e.g. [5]. The overall aim is to investigate possible mitigation schemes to improve the network robustness against remote base station interference, focusing primarily on synchronized TDD macro cells with semi-static DL/UL configurations. To this end, the guard period (GP) between DL and UL transmissions can already be increased in TDD-based long term evolution (TD-LTE) networks if an aggressor gNB can be detected and identified [6]. In general, the longer is the distance to the aggressor gNB, the higher is the number of UL symbols impacted at the victim gNB. As a concrete example, assuming subcarrier spacing (SCS) of 15 kHz mapping to a symbol duration of 66.7 μs, and cyclic prefix (CP) of 4.7 μs, and considering 100 km distance between the aggressor and the victim gNBs, the propagation delay corresponds already to approximately five OFDM symbols.

In general, the atmospheric ducting effect is highly dependent on temperature and humidity conditions and it is expected to last for hours when it occurs [6]. In 5G NR deployment scenarios, the impact of the troposphere bending is expected to be even more severe compared to TD-LTE networks due to the larger number of base stations required [7]. Hence, efficient mechanisms for remote interference management in NR (NR-RIM) should be studied and developed due to the large amount of possible interference sources with different propagation delays. Enhanced digital beamforming techniques can be expected to alleviate the remote interference problem, but they can not completely remove it.

The fundamental task of NR-RIM is to detect when the remote interference occurs, to identify the group of interfering

gNBs, and finally to measure the propagation delays between the aggressor and victim gNB or groups of gNBs. To this end, in order to detect and identify one or more interfering gNBs, a properly designed RIM reference signal (RIM-RS) can be adopted. Depending on the network configuration, a group of aggressor or victim gNBs, located in the same area where atmospheric ducting phenomenon occurs, may transmit the RIM-RS sequence within the same transmission period and same ID group. Due to channel reciprocity, the interference can be measured in the victim or aggressor side. In this context, it is commonly assumed that the whole network with synchronized macro cells has a common understanding on the DL and UL transmission and reception boundaries [5]. Thus, by allocating the RIM-RS to the last transmitted DL symbols, the receiving end can estimate the propagation delay under the assumed network synchronization.

This paper describes two feasible RIM-RS designs facilitating efficient detection of inter-gNB interference in the UL reception. The so-called one OFDM symbol (1OS) RIM-RS design builds on the 5G NR CSI-RS while the two OFDM symbol (2OS) RIM-RS is constructed similar to the LTE RIM-RS. The applicability of the two RIM-RS structures based on different time-frequency patterns, the necessary receiver processing framework, the achievable interference detection performance, the associated system overhead, and the impacts from the standardization point of view are all comprehensively addressed and discussed in the paper. To the best of our knowledge, no earlier article has studied and evaluated the most suitable RIM-RS designs for 5G NR networks noting the latest 3GPP specifications and RS requirements. The novelty of this paper is in describing the ducting phenomenon and related remote interference problem, comparison of different RS designs in terms of performance and standardization impact, and in providing the first detection performance results in the 5G NR RIM framework. Additionally, the obtained results show that 1OS RIM-RS provides better performance in scenarios with multiple interfering gNBs, despite using less physical resources than 2OS RIM-RS, while also allowing RS frequency multiplexing with the physical downlink shared channel (PDSCH) carrying user data.

The rest of the paper is organized as follows: Section II describes the considered 5G NR RIM-RS designs used to detect the remote inter-gNB interference. In Section III, the detection algorithm and considered performance metrics are described. Then, in Section IV, the detection performance of the considered RIM-RS designs is evaluated and analyzed. Finally, in Section V, the conclusions of this study are drawn.

II. Potential RIM Reference Signals for 5G NR

In TD-LTE networks, the RIM-RS adopts a repetitive structure similar to the physical random access channel (PRACH) preamble formats 2 and 3 [8], building on two identical copies of the LTE PRACH sequence, so that the detection can be done at OFDM symbol level in the receiver. Symbol level detection is considered also in 5G NR RIM studies to reduce the detector complexity in the gNB. The main difference between the RIM-RS and UL PRACH preamble designs is that the RIM-RS is assumed to occupy the full allocation bandwidth.

The existing NR reference signals support flexible configuration and could thus be considered as the starting point also for RIM-RS design. Considering the available synchronization signals for the remote interference detection, e.g., primary and secondary synchronization signals (PSS and SSS), we note that they may not be transparent to a user equipment (UE) trying to perform initial access procedures and, therefore, they are not considered for NR-RIM. The demodulation reference signal (DM-RS) is optimized for channel estimation in synchronized operation and it is never transmitted in the last DL symbol of a slot in 5G NR Release-15 [9], therefore, it is not considered in the NR RIM-RS development. On the other hand, especially when considering the backward compatibility, the NR CSI-RS which is defined only for DL can be mapped to any OFDM symbol within a slot and can be signaled to be transparent to a UE. The CSI-RS design also allows several resource allocation densities and may contain a repetitive structure in the time domain within one OFDM symbol due to the comb-like mapping to the frequency domain resources [9].

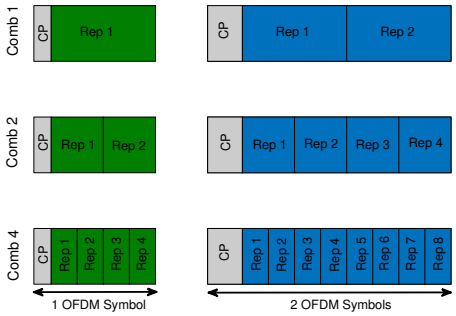

Fig. 2: Time domain resource allocation for the comb-1, comb-2, and comb-4 pilot patterns in the case of 1OS (left) and 2OS (right) RIM-RS designs.

A. NR RIM-RS Solutions with One and Two OFDM Symbols

1) 1OS RIM-RS: Based on the practical experience from TD-LTE networks, the duty cycle of the RIM-RS is expected to be low [5]. Then, the UE-specific 5G NR CSI-RS can form a good RIM-RS solution where the transmission periodicity can be flexibly configured. Based on its flexible configuration options [9], the one port CSI-RS supports several resource allocation densities per physical resource block. 5G NR Release-15 directly supports a comb-type mapping where the CSI-RS is allocated in every fourth subcarrier in the frequency domain (referred to as comb-4), which is then observed as 4-times repetitive structure in the time domain within one OFDM symbol, as illustrated in Fig. 2. The Release-15 CSI-RS design does not directly support comb-1 and comb-2 structures, but such extension is technically straight-forward and is thus considered in this paper. In general, considering the 1OS RIM-RS design, PDSCH data can be multiplexed within the same OFDM symbol in the case of comb-2 and comb-4 structures, which allows to further reduce the overhead caused by the 1OS RIM-RS. If the 1OS RIM-RS is transmitted without multiplexed PDSCH, power boosting of 6 dB for comb-4 pattern and 3 dB for comb-2 pattern is assumed to provide equal transmission power per OFDM symbol independent of the exact comb pattern.

2) 2OS RIM-RS: Similar to the LTE RIM-RS approach, the 2OS RIM-RS design contains two copies of the selected full-band PRACH sequence in the comb-1 case, as shown in Fig. 2, while supporting directly also comb-2 and comb-4 patterns. Note that in the case of 2OS RIM-RS design, the CP

length is doubled to align the number of transmitted samples with two CP-OFDM symbols. Clearly, this RIM-RS design can provide two times more transmitted energy and therefore provide higher detection probability, with twice the overhead. On the other hand, as it will be shown in Section IV, this also leads to a performance degradation when the number of simultaneously transmitted RIM-RS sequences is increased. The main drawback of the 2OS RIM-RS design is that it breaks the symbol alignment of the 5G NR physical layer and may cause significant inband interference unless special care in the bandwidth part filtering is considered. Also, because the symbol alignment is lost, it is not possible to frequency multiplex PDSCH data with the 2OS RIM-RS design.

B. Sequence Generation

The achievable performance in terms of the interference detection and false alarm probabilities for the two RIM-RS design candidates is highly related to the auto- and cross-correlation properties of the sequence transmitted within the RS. To facilitate good performance, pseudo-random sequences, $c(m)$, are deployed. They are generated by a length-31 Gold sequence that are generally widely used in 5G NR [9], [10]. The actual complex I/Q RIM-RS sequence, $r(m)$, of length M is QPSK modulated and is defined as $r(m) = 1/\sqrt{2}(1 - 2 \times c(2m)) + j/\sqrt{2}(1 - 2 \times c(2m+1))$.

Due to the good auto-correlation and cross-correlation properties, the selected pseudo-random sequences provide good detection sensitivity and are considered as baseline for the NR-RIM sequence generation [6]. It is assumed that there are in maximum eight different initialization values $c_{init} \in [5, 11, 22, 46, 74, 144, 194, 364]$ corresponding to eight different base sequences to be detected [5], with initialization values selected such that the cross-correlation coefficients are below 0.1 between the selected base sequences. Considering the frequency domain comb-1, comb-2, and comb-4 RS patterns illustrated in Fig. 2, three different sequence lengths ($M = 600$, $M = 300$ or $M = 150$) are evaluated, respectively.

III. Detection Algorithm and Performance Metrics

A. Detection Algorithm

The basic processing approach is to coherently combine the received RIM-RS repetitions within one detection window, after a sequence correlation in the frequency domain against a local replica of the RIM-RS signal. This local replica is generated by taking an FFT of length $2^{ceil(log_2 M)}$ of the RIM-RS sequence $r(m)$ for a given initialization value. Finally, the detection threshold for the correlation output is defined based on Chebyshevs inequality [11] to obtain the desired detection probability given the false alarm and error probability requirements. The most essential parameters of the detection algorithm for both RIM-RS designs are given in Table I.

The overall proposed detection methodology and the associated detection window locations are illustrated in Fig. 3. The detection window length, L_{symb}, corresponds to one UL CP-OFDM symbol and for simplicity, we assume that the RIM-RS and UL OFDM symbols have equal lengths. The delay window length, W_{symb}, corresponds to three OFDM symbols, and it defines the time interval within which the receiver is able to detect the RIM-RS given the expected propagation delay range of $[-L_{\text{symb}}, L_{\text{symb}}]$ [5]. The probability of capturing one full sequence transmitted with 2OS RIM-RS is higher than with 1OS RIM-RS due to the signal length. Therefore, depending on the RIM-RS design and sequence length, multiple detection windows will be needed within the delay window to improve the final detection performance. The detection window locations are aligned to the UL OFDM symbols as illustrated in Fig. 3. With 2OS RIM-RS design, it would be sufficient to use only two detection windows, corresponding to $W2$ and $W3$, but we have included a third window $W1$ to improve the detection reliability. For the 1OS RIM-RS design, at least three non-overlapping detection windows ($W1, W2, W3$) are required to detect any RS arriving within the delay window W_{symb}. However, in the worst case scenario the 1OS RIM-RS is exactly between the two detection windows and only 50% of the total energy can be captured within a single detection window. Therefore, with 1OS RIM-RS design, the detection performance can be further improved by introducing two additional overlapping windows ($EW1, EW2$) between detection window pairs $W1-W2$ and $W2-W3$ as illustrated in Fig. 3.

TABLE I: Physical layer parameterization and detection algorithm design

	Simulation assumptions
Channel model	AWGN with random phase rotation or TDL-E
Carrier frequency [GHz]	3.5
Bandwith [MHz]	20
Sub-carrier spacing [kHz]	30
Slot duration [ms]	0.5
Symbol duration (L_{symb})	FFT size + CP length = 1024 + 72
Antenna configuration	1 Tx $\times$ 1 Rx
Waveform	CP-OFDM

	Detection algorithm	
	1OS RIM-RS	2OS RIM-RS
Nº detection windows	5	3
Frequency pattern	Comb-type pattern: 1, 2 and 4	
Sequence type	Pseudo-random (length-31 Gold Sequence)	
Sequence length (M)	150, 300 and 600	
Detection window (L_{symb})	1 x L_{symb}	
Delay window (W_{symb})	3 x L_{symb}	
Delay of received RS	Uniformly distributed ϵ [-L_{symb},L_{symb}]	

B. Performance Metrics

One of the main purposes of the upcoming evaluations is to compare the two RIM-RS designs and define the minimum SNR requirements where the RIM-RS can still be detected under large propagation delays. To this end, the following three metrics are used in the evaluations [5]:

1) *The detection probability* is defined as the probability of detecting a sequence in a detection window given that the sequence is present in that detection window. As there are multiple detection windows within a delay window, if a sequence is detected in multiple adjacent detection windows, it is considered only once for the detection probability. Target value is 90%.

2) *The false alarm probability* is defined based on detecting any of the sequences in a detection window when no sequence was transmitted. Target value is 1%.

3) *The detection error probability* is defined as the probability that the detected sequence does not correspond to the possible set of active sequences actually arriving within the detection window. Target value is 1%.

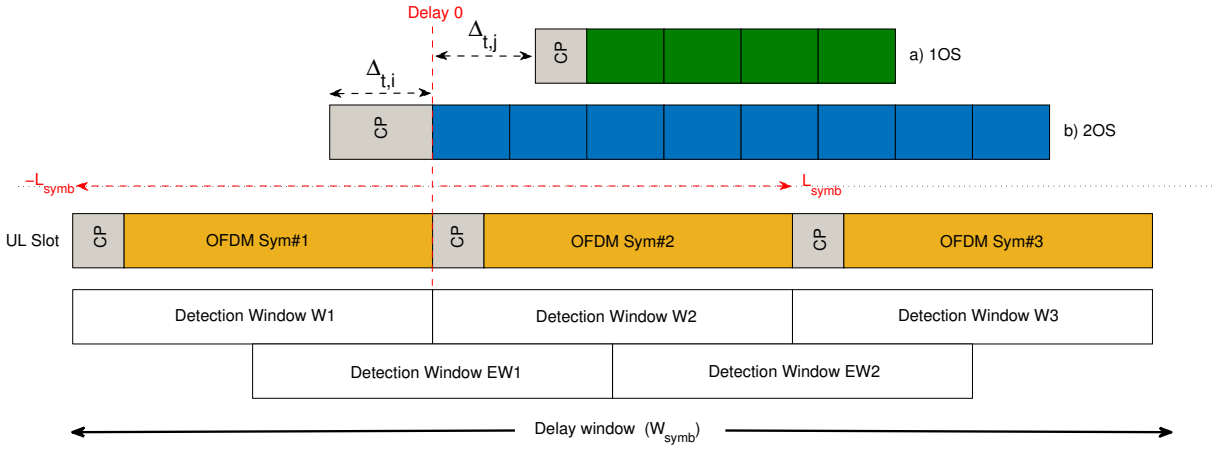

Fig. 3: Illustration of the detection algorithm used for both 5G NR RIM-RS designs. The arrival time $\Delta_{t,j}$ of one RIM-RS can be any value within [-L_{symb}, L_{symb}] wrt. the start of the reference detection window (e.g, $W2$). Non-overlapping detection windows ($W1, W2, W3$) are aligned to the UL OFDM symbols and two overlapping windows ($EW1, EW2$) are defined in the case of 1OS RIM-RS design. Delay window, W_{symb}, defines the time interval in which 1OS and 2OS RIM-RS can be detected.

IV. Remote Interference Detection Performance

In this section, the performance results for remote interference detection are presented, based on realistic link-level evaluations, considering both the 1OS and 2OS RIM-RS designs. All evaluations are performed using a 3GPP 5G NR standardization compliant radio link simulator based on the agreed simulation assumptions for the Release-16 NR-RIM study item [5]. Results are provided and analyzed for several sequence lengths and comb-type structures for both considered 5G NR RIM-RS designs. In the performance evaluations, an additive white Gaussian noise (AWGN) channel model with random phase rotation is assumed as a baseline to evaluate the detection performance of different 5G NR RIM-RS designs [5]. In addition, we extend the evaluations by including a tapped-delay-line (TDL-E) fading channel model [12], which models a line-of-sight channel with first tap following Ricean distribution with a K-factor of $K = 22$ dB and a root-mean-squared delay spread of 30 ns. Table I summarizes the exact link level parameters used in this study.

We first focus our evaluations on the scenario where only one remote gNB transmits a RIM-RS signal which is then received in the victim gNB with a random time offset. This simple scenario corresponds to the case C1 in Table II and it is the starting point of our studies to widely compare and calibrate the potential RIM-RS designs and detection performance, respectively. Secondly, the scenario where multiple gNBs transmit the same RIM-RS signal using the same RIM-RS sequence within the same transmission period is evaluated, which corresponds to the case C2 presented in Table II. Typically, when atmospheric ducting phenomenon occurs, it causes interference from a group of gNBs within a specific region towards a group of victim gNBs in another region, as illustrated already in Fig. 1. Therefore, it is considered beneficial to have a group of gNBs transmitting the same base sequence using the same ID group and within the same transmission period to improve the detection performance. Note that in the case of atmospheric ducting induced remote interference we are interested in detecting the region or a group of gNBs causing interference, whereas in general interference management context we typically want to identify the dominant interfering source, or an individual gNB.

TABLE II: Considered 5G NR RIM evaluation cases. N_{seq}: Maximum number of different base sequences used in the network, n: Number of different base sequences transmitted or arriving within a delay window, m: Number of gNBs transmitting a single base sequence. The total number of gNBs transmitting a RIM-RS and the number of sequences arriving to the receiver within a delay window is equal to $n \times m$.

	Case description	N_{seq}	n	m
C1	Single copy of a single sequence	1	1	1
C2	Multiple copies of a single sequence	1	1	10
C3	Single copy of multiple sequences	8	1, 2, 4, 8	1
C4	Multiple copies of multiple sequences	8	1, 2, 4, 8	10

TABLE III: Detection performance in terms of minimum SNR in case C1 (a single copy of a single RIM-RS sequence transmitted), comparing 1OS and 2OS RIM-RS designs with different comb-patterns in AWGN and TDL-E channels, assuming either non-power boosted operation (reference power) or power boosting for comb-2 and comb-4 patterns.

		AWGN		TDL-E	
		1OS RS	**2OS RS**	**1OS RS**	**2OS RS**
Reference Power	Comb-1	-13.5dB	-15.0 dB	-12.9 dB	-14.3 dB
	Comb-2	-10.0 dB	-11.2 dB	-9.2 dB	-10.4 dB
	Comb-4	-6.5 dB	-7.9 dB	-5.7 dB	-7.0 dB
Boosting	Comb-2	-12.9 dB	-14.2 dB	-12.2 dB	-13.3 dB
	Comb-4	-12.5 dB	-13.9 dB	-11.6 dB	-13.0 dB

Finally, to comprehensively evaluate the RIM-RS designs in the 5G NR-RIM framework, the performance with multiple different RIM-RS sequences transmitted from multiple gNBs is evaluated for cases C3 and C4 as defined in Table II. In the case of multiple RIM-RS sequences the cross-correlation properties of the selected sequences are highlighted and dominate the separation capability between different sequences mapping to either a gNB identity or a gNB group identity in cases C3 or C4, respectively. For these evaluations all RIM-RS sequences are transmitted using the same frequency domain resources. In all the cases and upcoming numerical results, we target 90% detection probability under the 1% false alarm rate and the 1% detection error rate, as discussed in Section III-B.

A. Performance with a Single Sequence Transmission

For the evaluation case C1, the obtained detection performance results are shown in Table III, in terms of the minimum

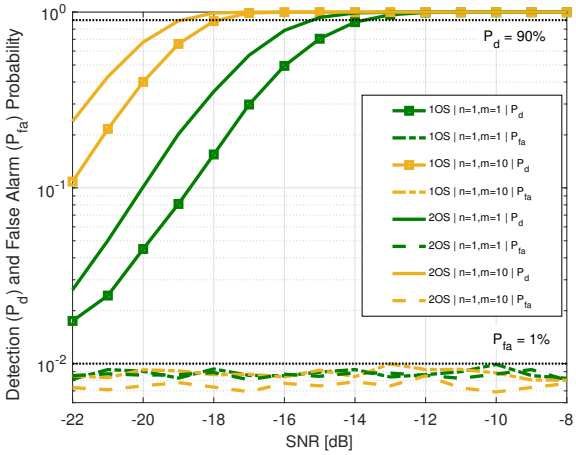

Fig. 4: Detection performance comparison using 1OS and 2OS RIM-RS with comb-1 structure in AWGN channel for cases C1 and C2.

received SNR to reach the target numbers of detection, misdetection and false alarm probabilities. The results are shown for five and three detection windows for the 1OS and 2OS RIM-RS designs, respectively. Based on additional evaluations, it was verified that increasing further the number of detection windows in case of 2OS RIM-RS does not provide any gain in the detection performance due to the longer RS. On the other hand, increasing the number of detection windows from three to five in case of 1OS RIM-RS, provides 1.7 dB gain in the detection performance. Further increasing the number of detection windows from five to nine provides 0.6 dB gain over five detection window case with the cost of higher detection complexity. The selected results corresponding to five detection windows with 1OS RIM-RS design provide in our opinion the best tradeoff between complexity and performance.

Based on results presented in Table III without power boosting, increasing the sequence length from 150 to 300 (comb-4 to comb-2), or from 300 to 600 (comb-2 to comb-1), provides a clear detection performance gain of approximately 3 dB for both RIM-RS designs. However, in these cases, comb-4 and comb-2 patterns are transmitted using only 25% and 50% of the total transmitted power obtained by comb-1 pattern. As discussed earlier, with 1OS RIM-RS design we can frequency multiplex PDSCH to the same OFDM symbol and the non-power boosted operation would thus correspond to this scenario. Then, by enabling 3 dB and 6 dB power boosting for comb-2 and comb-4 patterns, respectively, similar detection performance can be achieved for all comb-patterns. In addition, it was observed that all comb-shifts (cyclically shifting the comb-pattern in frequency domain) result in the same detection performance and, therefore, the RIM-RS supports two comb-shifts for comb-2 and four comb-shifts for comb-4 allowing to frequency multiplex different RIM-RSs. In general, in this simple scenario, 2OS RIM-RS achieves lower SNR operation point due to the doubled time duration and clearly increased overhead.

For the case C2, improvement in the detection performance compared to case C1 is achieved when the number of gNBs transmitting the same sequence is increased from 1 to 10, as shown in Fig. 4. This is intuitive, since when the number of gNBs transmitting the RIM-RS increases, also the probability of detecting at least one copy of the RIM-RS sequence increases. The maximum group size with which the performance still improves is an interesting future research topic. Fig. 4 also shows that increasing the number of gNBs transmitting the same sequence provides a similar detection enhancement for both RS structures (~ 4 dB) compared to case C1.

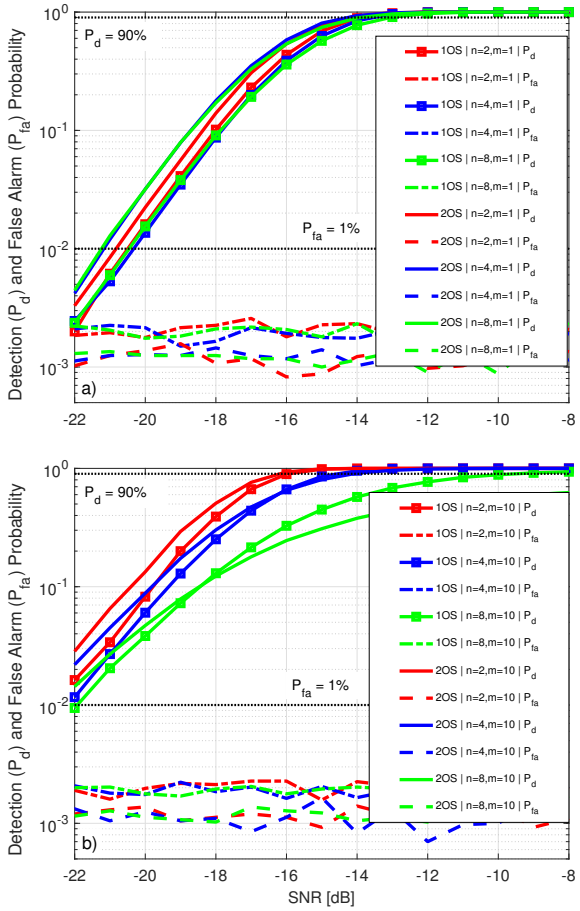

Fig. 5: Detection performance comparison using 1OS or 2OS RIM-RS with comb-1 structure in AWGN channel for cases a) C3 and b) C4.

B. Performance with Simultaneous Transmission of Multiple Sequences

Fig. 5 (a) depicts the detection probability for case C3, when different transmitted RIM-RS sequences are randomly chosen from the set of 8 possible base sequences. The receiver blindly detects the RIM-RS sequences and therefore the correlation is performed over the set of 8 local base sequences. This corresponds to the scenario where individual transmitting gNBs select different base sequences, e.g., based on higher level network signaling. In this case, the detection SNR threshold is higher than for case C1 when only one sequence arrives within the detection window. This is mainly because with the used receiver detection algorithm parameterization the false alarm rate is smaller for cases C3 and C4. The detection probability performance remains similar when increasing the number of sequences arriving within one delay window from 2 to 8 in case of 2OS RIM-RS, while the differences are somewhat larger for 1OS RIM-RS.

In real 5G NR deployment scenarios, the impact of the atmospheric ducting phenomenon can be severe due to the large number of base stations deployed in the network. With

TABLE IV: Detection performance summary, comparing 1OS and 2OS RIM-RS with comb-1 in AWGN and TDL-E channels. For the cases where 90% detection probability is not achieved, the detection probability at -10 dB SNR point is provided. For each case, the result for the RIM-RS design achieving lower detection SNR is highlighted in bold.

	AWGN		**TDL-E**	
	1OS RS	**2OS RS**	**1OS RS**	**2OS RS**
C1, m=1, n=1	-13.5 dB	**-15.0 dB**	-12.9 dB	**-14.3 dB**
C2, m=10, n=1	-17.9 dB	**-18.6 dB**	-19.3 dB	**-20.2 dB**
C3, m =1, n=1	-12.8 dB	**-14.1 dB**	-11.6 dB	**-13.2 dB**
C3, m =1, n=2	-13.9 dB	**-14.2 dB**	-12.9 dB	**-13.2 dB**
C3, m =1, n=4	-13.5 dB	**-14.3 dB**	-12.8 dB	**-13.5 dB**
C3, m =1, n=8	-13.1 dB	**-13.9 dB**	-12.3 dB	**-13.1 dB**
C4, m =10, n=1	-16.2 dB	**-17.0 dB**	-17.9 dB	**-18.9 dB**
C4, m =10, n=2	-15.9 dB	**-16.2 dB**	-16.5 dB	**-17.2 dB**
C4, m =10, n=4	**-14.5 dB**	-14.1 dB	**-14.69 dB**	-14.35 dB
C4, m =10, n=8	**-9.5 dB**	N/A,P_d=37%	**-8.25 dB**	N/A, P_d=46%

this in mind, Fig. 5 (b) shows that the detection probability decreases with increasing the number of different sequences arriving within a delay window when the number of transmitting gNBs per base sequence group is increased from 1 to 10. In the specific case of 8 different base sequences, the 2OS RIM-RS design is not able to achieve the 90% detection probability target value. This implies that with even larger gNB groups transmitting simultaneously or with even larger number of base sequences, the performance difference for the benefit of 1OS RIM-RS design can increase even further. Hence, in real deployment scenarios, the interference caused by multiple received sequences may increase faster with 2OS RIM-RS due to the longer time duration and higher overlap between sequences. This is another good topic for future studies.

The detection probability performance results are summarized in Table IV, showing results for the simulation cases C1, C2, C3, and C4. Although the 1OS RIM-RS design is not performing exactly as well as the 2OS RIM-RS design in the simpler scenarios (cases C1, C2, and C3), the performance of the 1OS exceeds the performance of 2OS RIM-RS design in the more challenging case C4, when there are 10 gNBs per group (m=10) and 4 or 8 different groups transmitting a different base sequence (n=4 or n=8, respectively).

Finally, to get further insight on the lowest realistic SNRs for remote interference detection, we next carry out some reference calculations. First, the distances between the aggressor and the victim gNBs are expected to be in the range of 64 km to 400 km based on trial results from TD-LTE networks [5], where the largest contribution to the interference was due to the base stations within a distance of 150 km. In the case of atmospheric ducting phenomenon, based on [4], the pathloss can be even smaller than free space path loss. Thus, to provide a conservative estimate of the SNR required to detect the remote interference over the distances described above, we use Friis transmission equation [13] for pathloss modeling. We further assume 3.5 GHz carrier frequency, -101 dBm noise power for the active band used by RIM-RS, and a typical base station transmission power of +43 dBm. Based on these assumptions, it follows that the distances of 64 km, 150 km, and 400 km correspond to SNR requirements of approximately 5.0 dB, -2.5 dB, and -11.0 dB, respectively. These results highlight that both RIM-RS designs can provide sufficient performance to detect remote radio interference under the atmospheric ducting phenomenon in all cases except case C4 with $m = 10$ and $n = 8$. Additionally, the 1OS RIM-RS design can facilitate remote interference detection up to distances of 340 km even in the most challenging case C4.

V. Conclusions

In this paper, remote radio interference stemming from atmospheric ducting phenomenon was studied, with particular emphasis on 5G NR networks. Two alternative reference signal structures for remote interference detection were described, together with the corresponding receiver processing framework. The obtained detection performance results show that the considered 2OS RIM-RS design provides slightly better performance than the 1OS RIM-RS design in simple scenarios where individual gNBs transmit different base sequences or only a few groups of gNBs simultaneously transmit different base sequences. As the number of base sequences or the number of simultaneously transmitting gNB groups is increased, the difference between the two designs decreases. Eventually, in cases where the number of gNBs per group equals 10 and 8 different base sequences are used for different groups, providing in total 80 simultaneously transmitting gNBs, the 1OS RIM-RS design using comb-1 structure provides already better performance than 20S RIM-RS. This implies that in practical 5G NR deployment scenarios, the 1OS RIM-RS could be more suitable than the 2OS RIM-RS design when increasing the number of gNBs transmitting different RIM-RS sequences, due to the shorter time duration and reduced probability for overlap between sequences in the receiver. In addition, the overhead of the 1OS RIM-RS design is smaller and allows to be frequency multiplexed with other DL user data. Based on the presented results, the maximum number of simultaneously transmitting gNBs together with the number of base sequences supported for RIM in 5G NR networks is an interesting point to address in future work, especially when noting the possibility to frequency multiplex different RIM-RS designs with comb-2 and comb-4 frequency patterns.

References

[1] M. Shafi et al., "5G: A Tutorial Overview of Standards, Trials, Challenges, Deployment, and Practice," *IEEE Journal on Selected Areas in Communications*, vol. 35, no. 6, pp. 1201–1221, 2017.

[2] J.D.Turton et al., "An introduction to radio ducting," *Meteorological Magazine*, vol. 117, no. 1393, pp. 245–254, 1988.

[3] Q. Liao et al., "Estimation of Surface Duct Using Ground-Based GPS Phase Delay and Propagation Loss," *Rem. Sen.*, vol. 10, no. 5, 2018.

[4] E. Dinc et al., "Channel model for the surface ducts: Large-scale pathloss, delay spread, and AOA," *IEEE Transactions on Antennas and Propagation*, vol. 63, no. 6, pp. 2728–2738, 2015.

[5] "3GPP TR 38866 V16.0.0, "Study on remote interference management for NR", Tech. Spec. Group Radio Access Network, Rel. 16," Dec 2018.

[6] A. Shen et al., "Monitoring and Avoidance of Atmospheric Duct on Interference Optimization in TD-LTE System," *Int. Conf. Signal And Information Processing, Networking & Computers*, pp. 36–45, 2017.

[7] E. Dahlman et al., "5G NR: The next generation wireless access technology," *Academic Press*, 2018.

[8] "3GPP TR 36211 V15.4.0, "Physical channels and modulation", Tech. Spec. Group Radio Access Network, Rel. 15," Dec 2018.

[9] "3GPP TR 38211 V15.4.0, "Physical channels and modulation", Tech. Spec. Group Radio Access Network, Rel. 15," Dec 2018.

[10] R. Gold et al., "Optimal binary sequences for spread spectrum multiplexing," *IEEE Transactions on information theory*, vol. 13, no. 4, pp. 619–621, 1967.

[11] P. Tchebichef et al., "Des valeurs moyennes," *Journal de Mathmatiques Pures et Appliques*, vol. 2, no. 12, pp. 177–184, 1867.

[12] "3GPP TR 38900 V15.0.0, "Study on channel model for frequency spectrum above 6 GHz", Tech. Spec. Group Radio Access Network, Rel. 15," June 2018.

[13] H. T. Friis, "A note on a simple transmission formula," *Proceedings of the IRE*, vol. 34, no. 5, pp. 254–256, 1946.